

Coherence of nonlinear Bloch dynamics of Bose-Einstein condensates in deep optical lattices

Ai-Xia Zhang(张爱霞), Wei Zhang(张薇), Jie Wang(王杰), Xiao-Wen Hu(胡潇文), Lai-Lai Mi(米来来), and Ju-Kui Xue(薛具奎)

Citation: Chin. Phys. B, 2024, 33 (**4**): 040305. DOI: 10.1088/1674-1056/ad1b46
Journal homepage: http://cpb.iphy.ac.cn; http://iopscience.iop.org/cpb

What follows is a list of articles you may be interested in

Effects of drive imbalance on the particle emission from a Bose-Einstein condensate in a one-dimensional lattice

Long-Quan Lai(赖龙泉) and Zhao Li(李照)
Chin. Phys. B, 2024, 33 (**3**): 030308. DOI: 10.1088/1674-1056/ad1172

Enhanced measurement precision with continuous interrogation during dynamical decoupling

Jun Zhang(张军), Peng Du(杜鹏), Lei Jing(敬雷), Peng Xu(徐鹏), Li You(尤力), and Wenxian Zhang(张文献)
Chin. Phys. B, 2024, 33 (**3**): 030301. DOI: 10.1088/1674-1056/ad1985

Dynamical nonlinear excitations induced by interaction quench in a two-dimensional box-trapped Bose-Einstein condensate

Zhen-Xia Niu(牛真霞) and Chao Gao(高超)
Chin. Phys. B, 2024, 33 (**2**): 020314. DOI: 10.1088/1674-1056/ad1179

Special breathing structures induced by bright solitons collision in a binary dipolar Bose-Einstein condensates

Gen Zhang(张根), Li-Zheng Lv(吕李政), Peng Gao(高鹏), and Zhan-Ying Yang(杨战营)
Chin. Phys. B, 2023, 32 (**11**): 110303. DOI: 10.1088/1674-1056/acf283

Nonlinear modes coupling of trapped spin-orbit coupled spin-1 Bose-Einstein condensates

Jie Wang(王杰), Jun-Cheng Liang(梁俊成), Zi-Fa Yu(鱼自发), An-Qing Zhang(张安庆),Ai-Xia Zhang(张爱霞), and Ju-Kui Xue(薛具奎)
Chin. Phys. B, 2023, 32 (**9**): 090305. DOI: 10.1088/1674-1056/accd53

Coherence of nonlinear Bloch dynamics of Bose–Einstein condensates in deep optical lattices

Ai-Xia Zhang(张爱霞)[†], Wei Zhang(张薇), Jie Wang(王杰), Xiao-Wen Hu(胡潇文), Lai-Lai Mi(米来来), and Ju-Kui Xue(薛具奎)[‡]

College of Physics and Electronics Engineering, Northwest Normal University, Lanzhou 730070, *China*

(Received 21 October 2023; revised manuscript received 31 December 2023; accepted manuscript online 5 January 2024)

Atomic interaction leads to dephasing and damping of Bloch oscillations (BOs) in optical lattices, which limits observation and applications of BOs. How to obtain persistent BOs is particularly important. Here, the nonlinear Bloch dynamics of the Bose–Einstein condensate with two-body and three-body interactions in deep optical lattices is studied. The damping rate induced by interactions is obtained. The damping induced by two-body interaction plays a dominant role, while the damping induced by three-body interaction is weak. However, when the two-body and three-body interactions satisfy a threshold, long-lived coherent BOs are observed. Furthermore, the Bloch dynamics with periodical modulation of linear force is studied. The frequencies of linear force corresponding to resonance and pseudoresonance are obtained, and rich dynamical phenomena, i.e., stable and strong BOs, drifting and dispersion of wave packet, are predicted. The controllable Bloch dynamics is provided with the periodic modulation of the linear force.

Keywords: Bose–Einstein condensate, atomic interaction, Bloch oscillations

PACS: 03.75.Lm, 03.75.Mn, 05.45.Yv **DOI:** 10.1088/1674-1056/ad1b46

1. Introduction

Bloch oscillations have been experimentally observed in superlattice systems[1–3] such as Bose–Einstein condensate (BEC) systems[4,5] and optical lattices[6–10] under constant external force. If a perturbation is applied to the Bloch state of a system, the Bloch wave of the BEC will suffer energy and dynamics instabilities.[11,12] The instability can only occur under certain condition, in which the interatomic interaction plays an important role. Both theoretical and experimental results show that the interatomic interaction has a strong effect on the energy band structure and dynamical instabilities[13] of the atoms in the optical lattices. It is well known that the atomic interaction leads to a dephasing and broadening of the wave function in momentum space, which causes a damping of the Bloch oscillations in coordinate space.[14–18] The damping rate increases with the strength of atomic interaction. This limits the application of Bloch oscillations (BOs), and how to obtain persistent BOs is particularly important. However, most of the current researches on this subject are limited to the consideration of interatomic two-body interaction. In fact, when the density of condensate is relatively small, the interatomic distance is much larger than the distance scale of the interatomic interaction, and the interatomic three-body interaction can be ignored. However, if the density of condensate is larger, the interatomic three-body interaction will also play a non-negligible role in the system.[19–24] Even if the strength of the three-body interaction force is small, it can have important effect on the properties of the condensate in the optical lattices, including the spatial modulation instability,[25] the energy and dynamics instabilities,[26] the band structure characteristics,[27] the tunneling dynamics,[28] and nonlinear properties.[29,30] In the experiment, the strengths of both the atomic interactions can be controlled by Feshbach resonance technology, providing a highly controllable ideal experiment platform for simulating condensed matter system. Then, if both two-body and three-body interactions present, how will the BOs in the one-dimensional optical lattices change? Can we obtain persistent BOs with combined effects of two-body and three-body interactions?

Further study shows that periodic linear force can also cause oscillatory motion or spatial localization of particles in periodic potential. This phenomenon known as dynamic localization is found within the framework of the tight-binding approximation.[31] Later studies have been carried out in cold atom systems in optical lattices[32] for coherent control of atoms[33] and for achieving superfluid-Mott-insulator phase transition.[34] Dynamic localization also occurs in optical lattice systems.[35–39] Periodic waveguide bending can simulate time-periodic linear force acting on quantum particles. Dynamic localization provides more opportunities to control dynamics of particle than BOs under constant external forces. Indeed, it can change the direction and average velocity of particles by changing the frequency of linear force. In contrast, a constant force leads only to oscillatory dynamics, and the amplitude of the force affects only the amplitude and frequency of the BOs. However, the nonlinear dynamic localization of

[†]Corresponding author. E-mail: zhangax@nwnu.edu.cn
[‡]Corresponding author. E-mail: xuejk@nwnu.edu.cn

© 2024 Chinese Physical Society and IOP Publishing Ltd

BECs with both two-body and three-body interactions in deep optical lattices under periodic linear force is still unclear.

To answer the above-mentioned questions, the nonlinear Bloch dynamics of BECs with both two-body and three-body interactions in one-dimensional deep optical lattices under constant and periodic linear force are studied systematically by means of the mean-field theory and the tight-binding approximation, combined with the variational principle. Under the action of a constant linear force, we show that the damping of BOs caused by two-body interaction plays a dominant role, while the damping caused by three-body interaction is weak. Furthermore, it is found that the persistent BOs can occur when both the two-body interaction and the three-body interaction exist at the same time and certain conditions are met. Under the action of a periodic modulated linear force, it is found that the system has rich Bloch dynamics, including strong BOs with large amplitude, drift of Bloch wave packet and significant dispersion of wave packet.

The organization of this paper is as follows: In Section 2, a model of BECs considering two-body and three-body interactions in inclined optical lattices is given and variational analysis is performed. In Section 3, the BOs of the system is analyzed and the influence of parameters of system on the BOs is discussed. In Section 4, we investigate the condition under which BOs can be maintained for a long time. In Section 5, the effective modulation of BOs under periodic linear force is discussed. Finally, in Section 6, a brief summary is given.

2. Model and variational approach

The dynamical properties of BECs in optical lattices with two-body and three-body interactions are considered. When the optical lattices are deep enough, the dynamics of the system with the presence of an external linear force can be described by the following discrete nonlinear Schrödinger equation under the tight-binding approximation:

$$\begin{aligned} \mathrm{i}\hbar\dot{a}_m = &-\frac{\tilde{J}}{2}(a_{m+1}+a_{m-1})+\tilde{g}|a_m|^2a_m \\ &+\tilde{\lambda}|a_m|^4a_m+\tilde{F}ma_m, \end{aligned} \tag{1}$$

where $\tilde{J}$ represents the tunneling coefficient between two adjacent lattices, $\tilde{g}$ represents the interatomic two-body interaction, $\tilde{\lambda}$ represents the interatomic three-body interaction, $\tilde{F}$ is the constant external force, and a_m represents the amplitude of the wave function of the condensate in the m-th lattice site. The coupling of the two-body interaction $\tilde{g}$, three-body interaction $\tilde{\lambda}$, the constant force $\tilde{F}$, and the tunneling coefficient $\tilde{J}$ will have complex effect on the dynamics of the BEC, which will be analyzed in detail in the following.

Using $t=[\hbar/\tilde{J}]t$ to readjust time t and dimensionless Eq. (1), we can obtain

$$\begin{aligned} \mathrm{i}\dot{a}_m = &-\frac{1}{2}(a_{m+1}+a_{m-1})+g|a_m|^2a_m \\ &+\lambda|a_m|^4a_m+Fma_m, \end{aligned} \tag{2}$$

where $g=\tilde{g}/\tilde{J}$, $\lambda=\tilde{\lambda}/\tilde{J}$, $F=\tilde{F}/\tilde{J}$. For current experiments, a variational estimate gives that the dimensionless parameters $g\sim 1$, $\lambda\sim 1$, and $F\sim 1$.[14] Indeed, those parameters can be tuned in a wide range. The external linear force F can be adjusted by modulating the lattice potential.[40] To avoid parametric and interband excitations, weak linear force is considered, i.e., $F<1$. The strength of the atomic interactions can be easily manipulated by the Feshbach resonance technology.[41] As discussed in Refs. [42–44], the nontrivial three-body effects can be expressed in terms of a single parameter of the hypervolume, and two-body interaction and three-body interaction with opposite signs in realistic van der Waals potential can be realized. Particularly, the independent controls of the two-body and three-body coupling constants are realized in a Rabi-coupled two-component BEC, allowing realization of two- and three-body interactions with opposite signs.[45] At the same time, using the Heisenberg equation of motion $\mathrm{i}\mathrm{d}a_m/\mathrm{d}t=\partial H/\partial a_m^*$, we can find the Hamiltonian of the system corresponding to Eq. (2) as

$$\begin{aligned} H = &-\frac{1}{2}\sum_m(a_ma_{m+1}^*+a_m^*a_{m+1})+\frac{g}{2}\sum_m|a_m|^4 \\ &+\frac{\lambda}{3}\sum_m|a_m|^6+F\sum_m m|a_m|^2. \end{aligned} \tag{3}$$

Next, we use the variational method[14,46] to study the influence of the coupling effect of system parameters on the dynamical characteristics of a BEC in one-dimensional optical lattices. We consider the dynamics of the wave packet, so the following normalized Gaussian trial wave function is used:

$$\begin{aligned} a_m(t) = &\frac{1}{R^{1/2}(\pi/2)^{1/4}} \\ &\times\exp\Big[-\frac{(m-\xi)^2}{R^2}+\mathrm{i}p(m-\xi)+\mathrm{i}\frac{\delta}{2}(m-\xi)^2\Big], \end{aligned} \tag{4}$$

where $R(t)$ and $\delta(t)$ represent the radius and the radius change rate of the Gaussian wave packet, respectively, and $\xi(t)$ and $p(t)$ represent the center-of-mass position and momentum of the wave packet, respectively. Substituting Eq. (4) into Eq. (3) and the Lagrangian density $L=\sum_m\frac{\mathrm{i}}{2}(\dot{a}_ma_m^*-a_m\dot{a}_m^*)-H$, we can reach

$$\begin{aligned} L = &p\dot{\xi}-\frac{1}{8}R^2\dot{\delta}+\mathrm{e}^{-\Theta}\cos p-\frac{g}{2\sqrt{\pi}R} \\ &-\frac{2\lambda}{3\sqrt{3}\pi R^2}-F\xi, \end{aligned} \tag{5}$$

where $\Theta=1/(2R^2)+\delta^2R^2/8$. To obtain Eq. (5), we replace the sums over m in the Lagrangian with integrals. Solving the Euler–Lagrangian equation $\frac{\mathrm{d}}{\mathrm{d}t}\frac{\partial}{\partial\dot{q}}=\frac{\partial L}{\partial q}$, the differential equations of motion related to variational parameters $q(t)=p,R,\xi,\delta$ can be obtained as follows:

$$\dot{p}=-F, \tag{6}$$

$$\dot{R} = \delta R \mathrm{e}^{-\Theta} \cos p, \tag{7}$$

$$\dot{\xi} = \mathrm{e}^{-\Theta} \sin p, \tag{8}$$

$$\dot{\delta} = -\mathrm{e}^{-\Theta} \cos p \left(\delta^2 - \frac{4}{R^4}\right) + \frac{2g}{\sqrt{\pi} R^3} + \frac{16\sqrt{3}\lambda}{9\pi R^4}. \tag{9}$$

The effective Hamiltonian of the system is

$$H = -\mathrm{e}^{-\Theta} \cos p + \frac{g}{2\sqrt{\pi} R} + \frac{2\lambda}{3\sqrt{3}\pi R^2} + F\xi. \tag{10}$$

The variational analysis with Gaussian ansatz (4) is widely used in studying the dynamics of interacting Bose gas. The variational analysis would be reasonable if the wave packet keeps Gaussian-like shape. The reasonability of our analytical results given by variational analysis will be confirmed by rich numerical simulations of the full GP equation (1). Based on the variational equations, when $F = 0$, we set the center of the wave packet at the origin of coordinate, that is, $\xi_0 = 0$. At this time, using the stationary solutions $\dot{q} = 0$, we can get $\delta_0 = 0$, $p_0 = 0$, which is the quasi-static state of the system when the external linear force is zero. Equations (6) and (8) respectively describe the temporal evolution of the momentum of the condensate and the velocity of the wave packet. The BOs of the system is mainly controlled by Eqs. (6) and (8). In the following sections we investigate Bloch dynamics of the system.

3. Bloch oscillation in tilted optical lattices

When $F \neq 0$, the optical lattices will be tilted, and $p(t) = p_0 - Ft$ can be obtained from Eq. (6). The external force will make the condensates do BOs, but the equations controlling the BOs are difficult to be solved analytically, so we use the fourth-order Runge–Kutta method to solve Eq. (2) numerically. The results of numerical simulation under different parameters are shown in Fig. 1.

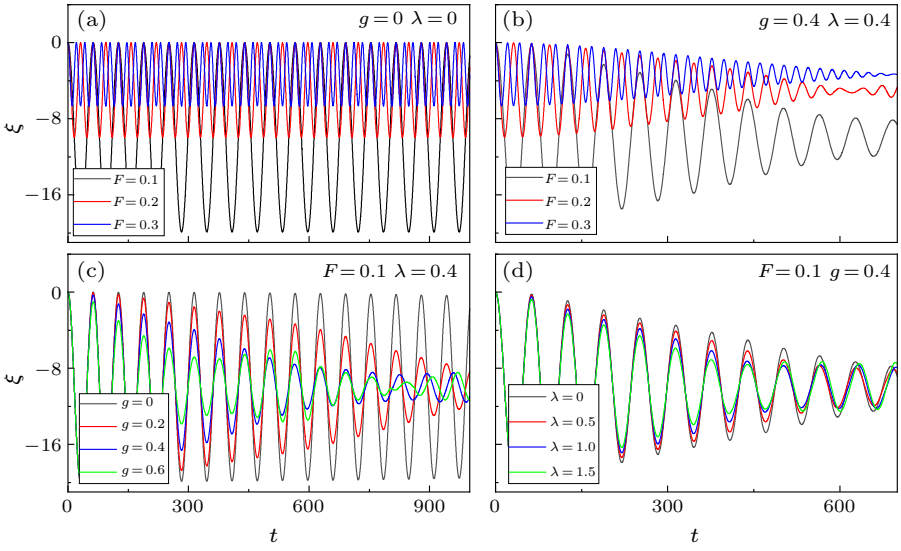


Fig. 1. BOs under different parameters F, g, and λ for $R = 10$.

As can be seen, the condensate exhibits an oscillatory mode. In the absence of atomic interaction, the oscillation is persistent and undamped [see Fig. 1(a)]. When the strength of interaction is fixed, the amplitude of the BOs decreases with the increase of the linear force F, and the frequency of the BOs increases with the increasing F [see Fig. 1(b)]. The interatomic interactions have no effect on the frequency of BOs. It is known that the interatomic interaction will cause the dephasing and broadening of the wave function in momentum space, which leads to damping of the BOs in coordinate space. The damping rate increases with the strength of atomic interaction. This law can be seen in Figs. 1(c) and 1(d). In addition, by comparing Fig. 1(c) with Fig. 1(d), it can be found that the damping rates of the two interactions on the BOs are different. The damping rate of BOs is high due to the two-body interaction g, while the damping effect of the three-body interaction λ on BOs is weak.

4. Long-lived BOs

As we mentioned above, the interatomic interactions could damp the BOs. Can BOs be sustained for a long time in the presence of interactions? Or, what is the condition for BOs to last for a long time? In order to solve this problem, we combine Eqs. (6)–(10) and get the following equation of oscillation for ξ:

$$\ddot{\xi} + \delta\chi\dot{\xi} + F^2\xi = F\left(H - \frac{g}{2\sqrt{\pi} R} - \frac{2\lambda}{3\sqrt{3}\pi R^2}\right). \tag{11}$$

Equation (11) describes the standard damped harmonic oscillator, where F^2 is the restoring force term, which also indicates that the natural period of the oscillation is $T_B = 2\pi/F$; $\chi = \frac{g}{2\sqrt{\pi} R} + \frac{4\sqrt{3}\lambda}{9\pi R^2}$ represents the damping rate of BOs. It

is obvious that the source of damping of BOs is the interatomic interaction. For fixed total number of atoms, different R means different effective atomic density, which is proportional to $1/R$. Hence, the wave packet width R modifies the effective atomic interaction energy [this is clearly shown in Eq. (10)], which results the modification of the damping rate χ. When R is fixed, Eq. (11) has an approximate solution $\xi \sim F^{-1}\mathrm{e}^{-1/2R^2}[\cos(Ft)\mathrm{e}^{-\frac{2}{R^2}\chi^2 t^2} - 1]$, which shows a damping oscillation. The damping rate is proportional to χ. From the expression of χ, it can be seen that the ratio of damping rate $\chi_2 = \frac{g}{2\sqrt{\pi}R}$ caused by two-body interaction to damping rate $\chi_3 = \frac{4\sqrt{3}\lambda}{9\pi R^2}$ caused by three-body interaction is $\frac{\chi_2}{\chi_3} = \frac{3\sqrt{3\pi}}{8}\frac{g}{\lambda}R$. When $g \sim \lambda$, it is obvious that $\chi_2/\chi_3 \gg 1$ ($R \gg 1$), that is, the damping caused by two-body interaction is much larger than that caused by three-body interaction. This is what we observed in Fig. 1. If $\chi \gg 0$, the oscillation will stop in a very short time. When $\chi = 0$, it means that there is no damping and the BOs can be sustained for a long time. Therefore, we can set $\chi = 0$ to obtain the condition for maintaining the long-lived BOs:

$$9\sqrt{\pi}gR + 8\sqrt{3}\lambda = 0. \tag{12}$$

Figure 2 presents the phase diagram for maintaining a long-lived BOs in the g–λ plane given by Eq. (12). Interatomic two-body interaction g and three-body interaction λ selected on the line satisfy $\chi = 0$, and the corresponding oscillations can be sustained for a long time. Here g and λ outside the line satisfy $\chi \gg 0$, and the corresponding oscillations will be damped for a short time. Note that, if only two-body term or three-body term presents, i.e., $\lambda = 0$ or $g = 0$, the damping rate will be proportional to g^2 or λ^2. Hence, in this case, the damping rate is independent of the sign of g or λ.

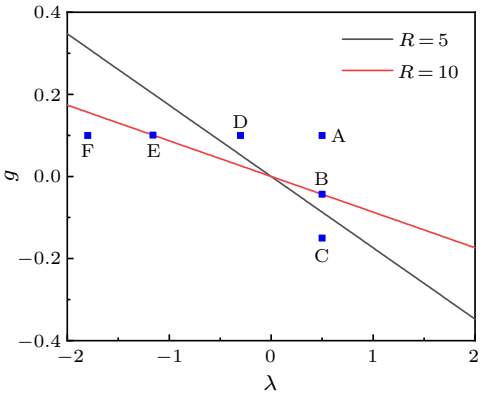


Fig. 2. Phase diagram for maintaining the long-lived BOs in g–λ plane.

In order to verify the accuracy of Eq. (2), the parameter values corresponding to the points A, B, C, D, E, and F in Fig. 2 are selected to numerical simulation of Eq. (2), and the corresponding results are presented in Fig. 3. When the point B or E is selected, the BOs have no tendency of damping, that is, the BOs can be maintained for a long time, which is well predicted by Eq. (12).

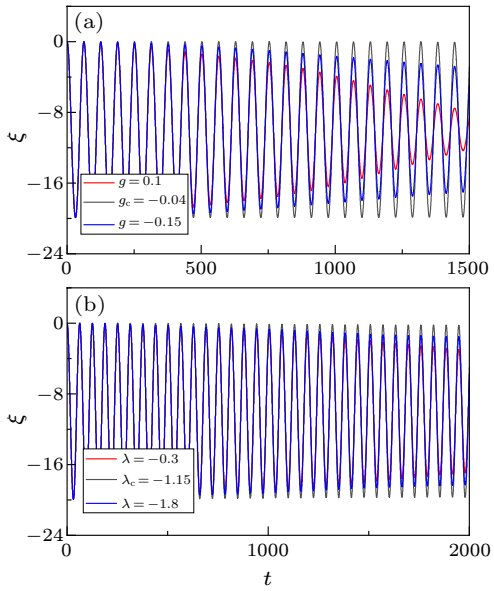


Fig. 3. BOs for parameters corresponding to the points (A, B, C, D, E, and F) marked in Fig. 2: (a) $\lambda = 0.5$, (b) $g = 0.1$. The other system parameters are $F = 0.1$ and $R = 10$.

5. Modulation of BOs

Assuming that the external force is not constant, we consider a linear force that varies periodically $F(t) = F_0 \sin(\omega t + \varphi)$, where F_0 and φ are the amplitude and the initial phase, ω is the frequency, $T = 2\pi/\omega$ is the period. Under the action of this external linear force, the variational equation of momentum (6) becomes

$$\dot{p} = -F_0 \sin(\omega t + \varphi). \tag{13}$$

Integrating the above formula, we get

$$p = p_0 + \frac{F_0}{\omega}[\cos(\omega t) - \cos\varphi]. \tag{14}$$

Substituting Eq. (14) into Eq. (8), we can obtain the dynamical equation of the center-of-mass of the wave packet as follows:

$$\dot{\xi} = \mathrm{e}^{-\Theta}\sin\left[p_0 + \frac{F_0}{\omega}\cos\omega t - \frac{F_0}{\omega}\cos\varphi\right]. \tag{15}$$

If the average velocity of the wave packet in a period T is zero, then the condition will read

$$\int_0^T \dot{\xi}\,\mathrm{d}t = 0. \tag{16}$$

In fact, when Eq. (16) is satisfied, dynamic localization of the wave packet will occur,[31] then the shape of wave packet will recover after each cycle, that is, there is no dispersion. From Eq. (16), we can reach

$$\sin\left(\frac{F_0}{\omega}\cos\varphi - p_0\right) \times J_0\left(\frac{F_0}{\omega}\right) = 0, \tag{17}$$

where $J_0(\cdot)$ is the first kind of zero-order Bessel function. When Eq. (17) is satisfied, the resonant frequency of dynamic

localization $\omega = \omega_k$ can be obtained. Setting $J_0(F_0/\omega) = 0$, ω_k can be approximately provided by $\omega_k = F_0/\nu$, where $\nu_1 \approx 2.405$, $\nu_2 \approx 5.520$, etc., are of the zeros of $J_0(\nu)$. When the frequency is ω_k, the wave packet changes periodically in time, i.e., a stable BOs occurs. Condition (17) is also satisfied in the case $(F_0/\omega)\cos\varphi - p_0 = n\pi$, that is, the $\omega = \omega_n = \frac{F_0\cos\varphi}{n\pi + p_0}$, with n being an integer. Here ω_n depends on the initial momentum p_0 and the initial phase of the external force φ, so the oscillation of the wave packet at $\omega = \omega_n$ will accompany the effective dispersion. Thus the frequency ω_n is not the true resonant frequency corresponding to dynamic localization. To distinguish it from $\omega = \omega_k$, we refer to $\omega = \omega_n$ as the pseudoresonant frequency. When $n = 0$ and $\varphi = 0$, the initial momentum, the external linear force, and the pseudoresonant frequency should satisfy $\omega = \omega_n = F_0/p_0$. When the values of p_0 and n are small, ω_k and ω_n alternate, that is, a pseudoresonance between the two resonances can exist.

In order to confirm the results predicted by the theory, the parameter values of points A and E in Fig. 2 are selected, and we perform the direct numerical simulations of Eq. (2). Here, we set $F_0 = 0.2$ and $\varphi = 0$, i.e.,

$$F(t) = F_0 \sin(\omega t). \tag{18}$$

Figures 4 (the parameters corresponding point A in Fig. 2 are used) and 5 (the parameters corresponding point E in Fig. 2 are used) show the temporal evolutions for oscillatory mode of a Gaussian wave packet under different frequencies of the periodic linear force. Figures 4(a), 4(d), 5(a), and 5(d) show the evolutions of the wave packet at the resonant frequencies. At resonant frequencies, the dynamics of wave packets show strong BOs with larger amplitudes. At the pseudoresonant frequencies [Figs. 4(b), 4(e), 5(b), and 5(e)], the dispersion of wave packet occurs and we can see the obvious diffusion. Figures 4(c), 4(f), 5(c), and 5(f) show the very obvious drift of the wave packet at non-resonant frequencies. In this case, Eq. (16) is not satisfied, such as $\int_0^T \dot{\xi}\,\mathrm{d}t < 0$, the average velocity of the wave packet in a period T is negative. Then, the wave packet can not recover its initial position after each cycle and has a drift towards $-m$ direction. This results in the drift of the wave packet at non-resonant frequencies. The resonance and pseudoresonance frequencies predicted by theory are proved to be correct by numerical simulations. Comparing Figs. 4 and 5, it can be clearly seen that due to the dephasing, in Fig. 4 [where the condition (12) is not satisfied], the wave packet will experience diffusion effect even at resonant frequencies [Figs. 4(a) and 4(d)]. However, when the condition (12) is satisfied (Fig. 5), the dispersion effect is significant suppression, especially at the pseudoresonant frequencies [Figs. 5(b) and 5(e)]. Furthermore, comparing the dynamics of wave packet at the first set of frequencies $\omega_k = F_0/\nu_1$ (the first rows in the Figs. 4 and 5) and the dynamics of wave packet at the second set of frequencies $\omega_k = F_0/\nu_2$ (the second rows in the Figs. 4 and 5), we can see that the smaller the modulation frequency is, the more complex the corresponding oscillatory mode works. The direction of movement of wave packet changes more times in an oscillation period. Because the wave packet oscillates and drags at the same time, the wave packet drags more slowly at a smaller non-resonant frequency [Figs. 4(f) and 5(f)]. The dynamics of wave packet is well controlled by the periodic modulation of the external force.

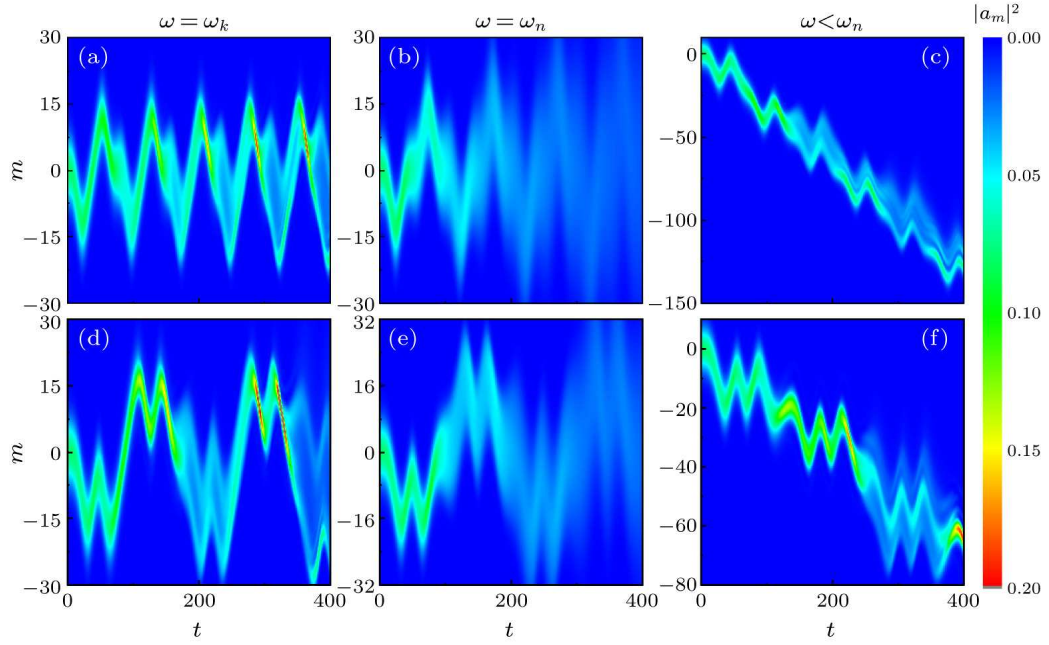


Fig. 4. Temporal evolutions of Gaussian wave packet: (a) $\omega = \omega_k = F_0/\nu_1 = 0.0832$, (b) $\omega = \omega_n = F_0/\pi = 0.0637$, (c) $\omega = 0.0450$, (d) $\omega = \omega_k = F_0/\nu_2 = 0.0362$, (e) $\omega = \omega_n = F_0/2\pi = 0.0318$, (f) $\omega = 0.0250$. The other system parameters are $p_0 = 0$, $g = 0.1$, $\lambda = 0.5$, $F_0 = 0.2$, and $R = 10$.

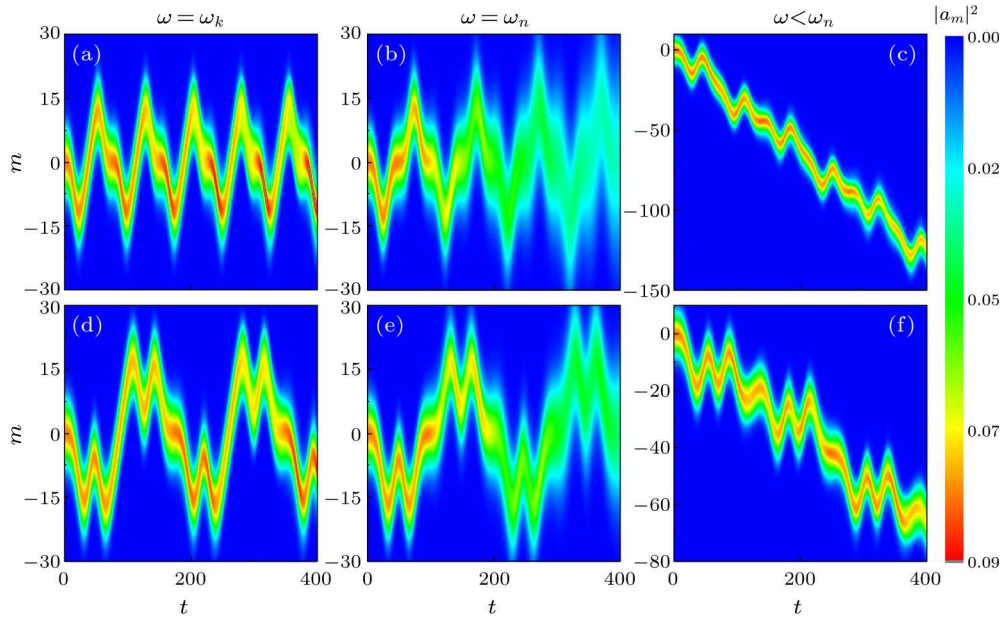


Fig. 5. Temporal evolutions of Gaussian wave packet: (a) $\omega = \omega_k = F_0/\nu_1 = 0.0832$, (b) $\omega = \omega_n = F_0/\pi = 0.0637$, (c) $\omega = 0.0450$, (d) $\omega = \omega_k = F_0/\nu_2 = 0.0362$, (e) $\omega = \omega_n = F_0/2\pi = 0.0318$, (f) $\omega = 0.0250$. The other system parameters are $p_0 = 0$, $g = 0.1$, $\lambda = -1.15$, $F_0 = 0.2$, and $R = 10$.

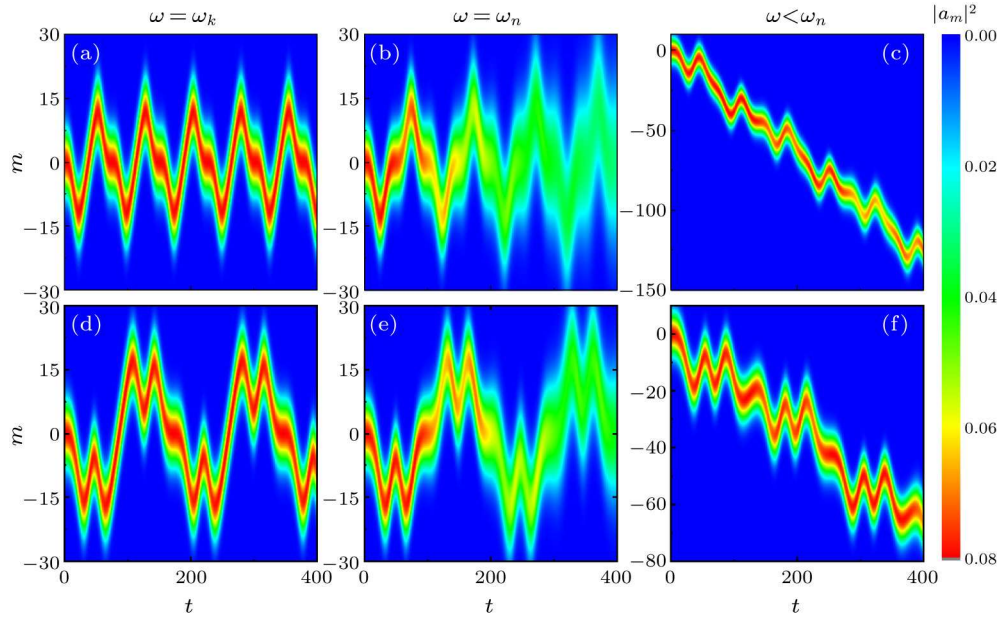


Fig. 6. The same as Fig. 5 but with $g = 0$ and $\lambda = 0$.

To further confirm the affect of atomic interactions on Bloch dynamics with a periodic external force, Fig. 6 shows the results in a linear case. When the atomic interactions are absent, the wave packet does persistent Bloch oscillation, and the diffusion is very weak as the wave packet oscillating and dragging. Especially, the dispersion effect at the pseudoresonant frequency is significantly suppressed.

6. Conclusion

We provide a model to explore and manipulate the nonlinear Bloch dynamics. Considering both two-body and three-body interactions, the nonlinear Bloch dynamics of BECs in deep optical lattices under external linear force is studied analytically and numerically. The destruction effects of two-body and three-body interactions on Bloch dynamics are discussed. The physical mechanism for maintaining long-lived BOs is revealed. The atom–atom interactions cause the BOs to be damped, while the damping rates of the oscillations are different for the two-body interaction and three-body interaction. Interestingly, when the two-body and three-body interactions satisfy a certain relationship, the long-lived BOs can be maintained. We also discuss the influence of the periodic modulation of the linear force on the Bloch dynamics. Compared with

the traditional BOs under a static linear force, the dynamic localization under periodic modulated linear force provides more ideas for controlling the particle dynamics. We provide an efficient scheme to explore and manipulate the Bloch dynamics in a controllable way.

Acknowledgments

Project supported by the National Natural Science Foundation of China (Grant Nos. 12264045, 12164042, 11764039, 11847304, and 11865014), the Natural Science Foundation of Gansu Province (Grant No. 17JR5RA07620JR5RA526), the Scientific Research Project of Gansu Higher Education (Grant No. 2016A-005), the Innovation Capability Enhancement Project of Gansu Higher Education (Grant Nos. 2020A-146 and 2019A-014), and the Creation of Science and Technology of Northwest Normal University (Grant No. NWNU-LKQN-18-33).

References

[1] Feldmann J, Leo K, ShahJ, Miller D A B, Cunningham J E, Meier T, von Plessen G, Schulze A, Thomas P and Schmitt-Rink S 1992 *Phys. Rev. B* **46** 7252
[2] Leo K, Bolivar P H, Brggemann F, Schwedler R and Khler K 1992 *Solid State Commun.* **84** 943
[3] Waschke C, Roskos H G, Schwedler R, Leo K, Kurz H and Khler K 1993 *Phys. Rev. Lett.* **70** 3319
[4] Morsch O, Mller J H, Cristiani M, Ciampini D and Arimondo E 2001 *Phys. Rev. Lett.* **87** 140402
[5] Cristiani M, Morsch O, Mller J H, Ciampini D and Arimondo E 2002 *Phys. Rev. A* **65** 063612
[6] Peschel U, Pertsch T and Lederer F 1998 *Opt. Lett.* **23** 1701
[7] Pertsch T, Dannberg P, Elflein W, Bruer A and Lederer F 1999 *Phys. Rev. Lett.* **83** 4752
[8] Morandotti R, Peschel U, Aitchison J S, Eisenberg H S and Silberberg Y 1999 *Phys. Rev. Lett.* **83** 4756
[9] Sapienza R, Costantino P, Wiersma D, Ghulinyan M, Oton C J and Pavesi L 2003 *Phys. Rev. Lett.* **91** 263902
[10] Trompeter H, Krolikowski W, Neshev D N, Desyatnikov A S, Sukhorukov A A, Kivshar Y S, Pertsch T, Peschel U and Lederer F 2006 *Phys. Rev. Lett.* **96** 053903
[11] Wu B and Niu Q 2003 *New J. Phys.* **5** 104
[12] Machholm M, Pethick C J and Smith H 2003 *Phys. Rev. A* **67** 053613
[13] Liu W M, Wu B and Niu Q 2000 *Phys. Rev. Lett.* **84** 2294
[14] Trombettoni A and Smerzi A 2001 *Phys. Rev. Lett.* **86** 2353
[15] Gustavsson M, Haller E, Mark M J, Danzl J G, Rojas-Kopeinig G and Nägerl H C 2008 *Phys. Rev. Lett.* **100** 080404
[16] Fattori M, D'Errico C, Roati G, Zaccanti M, Jona-Lasinio M, Modugno M, Inguscio M and Modugno G 2008 *Phys. Rev. Lett.* **100** 080405
[17] Witthaut D, Werder M, Mossmann S and Korsch H J 2005 *Phys. Rev. E* **71** 036625
[18] Buchleitner A and Kolovsky A R 2003 *Phys. Rev. Lett.* **91** 253002
[19] Gammal A, Frederico T, Tomio L and Abdullaev F Kh 2000 *Phys. Lett. A* **267** 305
[20] Abdullaev F K, Gammal A, Tomio L and Frederico T 2001 *Phys. Rev. A* **63** 043604
[21] Bulgac A 2002 *Phys. Rev. Lett.* **89** 050402
[22] Khler T 2002 *Phys. Rev. Lett.* **89** 210404
[23] Leanhardt A E, Chikkatur A P, Kielpinski D, Shin Y, Gustavson T L, Ketterle W and Pritchard D E 2002 *Phys. Rev. Lett.* **89** 040401
[24] Pieri P and Strinati G C 2003 *Phys. Rev. Lett.* **91** 030401
[25] Zhang W, Wright E M, Pu H and Meystre P 2003 *Phys. Rev. A* **68** 023605
[26] Akhmediev N, Das M P and Vagov A V 1999 *Int. J. Mod. Phys. B* **13** 625
[27] Zhang A X and Xue J K 2007 *Phys. Rev. A* **75** 013624
[28] Abdullaev F K and Salerno M 2005 *Phys. Rev. A* **72** 033617
[29] Merhasin I M, Gisin B V, Driben R and Malomed B A 2005 *Phys. Rev. E* **71** 016613
[30] Mihalache D, Mazilu D, Lederer F, Kartashov Y V, Crasovan L C, Torner L and Malomed B A 2006 *Phys. Rev. Lett.* **97** 073904
[31] Dunlap D H and Kenkre V M 1986 *Phys. Rev. B* **34** 3625
[32] Holthaus M 1992 *Phys. Rev. Lett.* **69** 351
[33] Zenesini A, Lignier H, Ciampini D, Morsch O and Arimondo E 2009 *Phys. Rev. Lett.* **102** 100403
[34] Eckardt A, Weiss C and Holthaus M 2005 *Phys. Rev. Lett.* **95** 260404
[35] Longhi S, Marangoni M, Lobino M, Ramponi R, Laporta P, Cianci E and Foglietti V 2006 *Phys. Rev. Lett.* **96** 243901
[36] Iyer R, Aitchison J S, Wan J, Dignam M M and de Sterke C M 2007 *Opt. Express* **15** 3212
[37] Dreisow F, Heinrich M, Szameit A, Dring S, Nolte S, Tnnermann A, Fahr S and Lederer F 2008 *Opt. Express* **16** 3474
[38] Arlinghaus S, Langemeyer M and Holthaus M 2011 *Dynamical Tunneling: Theory and Experiment* (New York: Taylor & Francis) p. 289
[39] Madison K W, Fischer M C, Diener R B, Niu Q and Raizen M G 1998 *Phys. Rev. Lett.* **81** 5093
[40] Wintersperger K, Bukov M, Nager J, Lellouch S, Demler E, Schneider U, Bloch I, Goldman N and Aidelsburger M 2020 *Phys. Rev. X* **10** 011030
[41] Ha L C, Hung C L, Zhang X, Eismann U, Tung S K and Chin C 2013 *Phys. Rev. Lett.* **110** 145302
[42] Mestrom P M A, Colussi V E, Secker T, Groeneveld G P and Kokkelmans S J J M F 2020 *Phys. Rev. Lett.* **124** 143401
[43] Tan S 2008 *Phys. Rev. A* **78** 013636
[44] Zhu S and Tan S 2017 arXiv:1710.04147 [cond-mat.quant-gas]
[45] Hammond A, Lavoine L and Bourdel T 2022 *Phys. Rev. Lett.* **128** 083401
[46] Kurizki G, Kozhekin A E, Opatrny T and Malomed B A 2001 *Prog. Opt.* **42** 93